58906-00-105

ANL/MSD/CP-92084

CONF-961076--2

Probing of the Phase Diagram of Layered High T_c Superconductors by Monte Carlo Simulations

A.E. Koshelev

Materials Science Division, Argonne National Laboratory, Argonne, IL 60439

and

Institute of Solid State Physics, Chernogolovka, Moscow District, 142432, Russia

Proceedings of the 9th International Symposium on Superconductivity, Sapporo, Japan, October 21-24, 1996

*Work supported by the U.S. Department of Energy, BES-Materials Sciences under contract #W-31-109-ENG-38 and by the National Science Foundation Office of Science and Technology Centers for Superconductivity under contract #DMR91-20000.

PROBING OF THE PHASE DIAGRAM OF LAYERED HIGH T_C SUPERCONDUCTORS BY MONTE CARLO SIMULATIONS

A.E.Koshelev

Material Science Division, Argonne National Laboratory, Argonne, IL 60439 and Institute of Solid State Physics, Chernogolovka, Moscow District, 142432, Russia

ABSTRACT

The phase diagram of layered superconductors is explored by Monte-Carlo simulations of the three-dimensional uniformly frustrated XY model. Two regimes of behavior were observed depending on the anisotropy. At high anisotropy, the melting occurs as a strong first order phase transition and is accompanied by the destruction of vortex lines and the disappearance of superconductivity along the field direction. At low anisotropies melting is shallow and the vortex crystal melts into a liquid of vortex lines with superconductivity along the field direction.

KEY WORDS: layered superconductors, vortex lattice melting, phase diagram

INTRODUCTION

The thermodynamic and transport properties of Type II superconductors in magnetic field are essentially properties of the "vortex matter". A peculiarity of high T_c superconductors is a very high amplitude of thermal fluctuations in the vortex state. This leads to the destruction of the low temperature vortex crystal state well below the mean field upper critical field. Fluctuations are especially strong in layered materials where the vortex lines consist of weakly coupled "pancakes" due to weak coupling between superconducting planes .

Understanding the field-temperature phase diagram of layered superconductors is very important for both fundamental science and applications. At low fields the vortex lattice has to melt into a liquid of well defined vortex lines. Whether or not the line liqud phase differs qualitatively from the normal phase is the fundamental and unresolved question (see, e.g. [1,2]). If it represents a distinct phase than another phase transition should exist at higher temperatures, at which this intermediate phase transforms into the normal phase. It is also of fundamental importance to know if the line liquid preserves phase coherence along the field? Exact positions of the possible transitions in the field-temperature plane and their thermodynamic characteristics are unknown at present. Quantitative analysis is possible only by large scale numerical simulations.

Experimentally, a sharp transition has been observed in clean high-T_c samples at which both the resistance [3] and the equilibrium magnetization [4] jump discontinuously . While this transition has generally been interpreted as a first order melting of the vortex line lattice, the apparent entropy jump (as much as 2-6 k_B per vortex per layer in $Bi_2Sr_2CaCu_2O_x$ near the zero field transition [4]) seems to be larger than such a melting transition would suggest.

The melting transition at low fields can be adequately described by a simple model of vortex lines with pair interactions [5]. However this model is not sufficient for investigating the processes of thermal disintegration of vortex lines and crossover/transition to the normal phase. To study these issues, one has to use some field model, in which vortex lines appear as singularities in the distribution of the order parameter. The simplest realization of such a field model is the model of interacting phases (uniformly frustrated XY model) [6,7]. This model keeps the most essential phase degree of freedom of the superconductor and neglects less important fluctuations of the order parameter amplitude and the field. As far as thermodynamic properties are concerned the uniformly frustrated XY model is equivalent to the three dimensional Josephson junction array. In addition, dynamic simulations of the latter model [9,10] allow investigation the electric transport near the transitions. The important

To be published in:
Proceedings of the 9th International Symposium on Superconductivity (ISS '96)

parameter of the model is the fraction of grid sites b filled by vortices (see Section 2), which has to be very small to provide a realistic description of the superconductor in the London limit. Simulations show that for $b < 1/15$ the vortex crystal transforms into the normal state through the intermediate line liquid phase in the isotropic [6] and moderately anisotropic [8] cases. On the other hand for larger filling factors ($b = 1/6$), the vortex crystal was found to transform directly into the normal phase as a result of a strong first order phase transition [7,10]. Alternatively, the phase transitions in the London regime have been explored by the "lines and loops" model [11–13], which is dual to the frustrated XY model with the Villain type of interaction between neighboring phases. Very similar behavior have been found, i.e., direct melting into the normal state for moderate b, $b = 1/4, 1/8$ [11], and transitions through the intermediate phase for very small b [12,13].

The vortex phases in layered superconductors was also investigated within the so-called the lowest Landau level (LLL) approximation which is valid near the upper critical field H_{c2} [14,15]. In the parameter range corresponding to the compound $YBa_2Cu_3O_7$ [14] the melting was found to be weakly first order phase transition. The liquid phase emerging above the melting transition does not have superconductivity along the field direction and merges smoothly into the normal state.

In spite of considerable numerical efforts, the issues of the thermodynamics of the transitions and their evolution with increasing anisotropy still remain open. In this paper, we extend the simulations of the uniformly frustrated XY model to monitor the evolution of the phase diagram with the increase of the anisotropy parameter Γ. In the London limit, thermodynamic properties depend only upon the reduced magnetic field $B\Gamma s^2/\Phi_0$, which means that an increase of anisotropy is equivalent to an increase of magnetic field. We use realistic parameters in order to extract quantitative information about the phase transitions and the nature of the vortex phases.

DESCRIPTION OF THE MODEL

Phenomenologically, any state of a layered superconducor is characterized by a distribution of the complex order parameter $\Psi_n = \rho_n \exp(i\phi_n)$ and the vector-potential $\mathbf{A}$. At fields much smaller than the upper critical field (London regime), the amplitude of the order parameter ρ_n is suppressed only in the vicinity of the vortex cores, i.e. over a very small fraction of the total volume. In this regime a simplified description in terms of phase ϕ_n and the vector-potential distributions is possible. Vortex positions $\mathbf{R}_{in}$ are defined as singular points in the phase distribution, $(\nabla_x\nabla_y - \nabla_y\nabla_x)\,\phi_n = \sum_j \delta(\mathbf{r} - \mathbf{R}_{in})$. The energy of a superconductor in the London regime can be written as

$$E[\phi_n, \mathbf{A}] = N_v\varepsilon_{core} + \sum_n \int d^2r \left[\frac{J}{2}\left(\nabla\phi_n - \frac{2\pi s}{\Phi_0}\mathbf{A}\right)^2 + E_J\left(1 - \cos\left(\phi_{n+1} - \phi_n - \frac{2\pi s}{\Phi_0}A_z\right)\right)\right] + \int d^3r \frac{B^2}{8\pi} \quad (1)$$

where N_v is the total number of pancake vortices, ε_{core} is the energy of the core region, and the integral in the second term avoids the core regions. The system is characterized by two energetic parameters: the phase stiffness constant J and the Josephson coupling energy E_J. These parameters can be connected with experimentally accessible parameters by the relations

$$J = \frac{s\Phi_0^2}{\pi(4\pi\lambda)^2};\quad E_J = \frac{\Phi_0^2}{s\pi(4\pi\lambda\gamma)^2}$$

where s is the interlayer spacing, λ is the London penetration depth, and γ is the anisotropy factor. In general, the vector potential consists of the contribution coming from the external magnetic field $\mathbf{A}_B$ and the extra contribution coming from supercurrents $\mathbf{A}_j$. At high fields the supercurrent contribution is small and influences only weakly the properties of the "vortex matter." Keeping only $\mathbf{A}_B$, we obtain the "frozen field" approximation. In this approximation, the system is totally characterized by the phase distribution and the statistical mechanics is determined by the partition function $Z = \int D\phi_n \exp(-E[\phi_n, \mathbf{A_B}]/T)$. From the structure of the free energy functional (1) one can derive a very important scaling property of the free energy per layer, $f = -(T/S)\ln Z$. A natural energy scale of the problem is the

phase stiffness J. It can be also observed that the only relevant field scale is the crossover field $B_{cr} = \Phi_0/\Gamma s^2$ with $\Gamma = \gamma^2$, and the field contribution to the free energy $f_B = f(B) - f(0)$ can be represented as

$$f_B = \frac{B}{\Phi_0}\left(\varepsilon_{core} + Jg_{sc}(\frac{T}{J}, \frac{B\Gamma s^2}{\Phi_0})\right). \tag{2}$$

Thermodynamic properties are determined by the scaling function g_{sc}, which depends upon the dimensionless temperature and field. Important consequence of the scaling (2) is that thermodynamic properties of superconductors do not depend separately upon field and anisotropy but only upon the combination $\frac{B\Gamma s^2}{\Phi_0}$. This means that the phase diagram plotted in coordinates T/J and $\frac{B\Gamma s^2}{\Phi_0}$ has to be universal for all layered superconductors.

For numerical simulations one has to discretize the continuum distribution, $\phi_n(\mathbf{r}) \to \phi(\mathbf{n})$ with $\mathbf{n} = (n_x, n_y, n_z)$, where the continuous coordinates $\mathbf{r} = (x, y)$ have been replaced by the indices (n_x, n_y) and the index n is replaced by n_z. The phases $\phi(\mathbf{n})$ are defined at the sites of the rectangle $1 \le n_x, n_y \le N_\perp, 1 \le n_z \le N_z$ with periodic boundary conditions in all directions. The energy of interacting phases is given by

$$E = \sum_{\mathbf{n}}\left(\sum_{\alpha=(x,y)} V\left(\phi(\mathbf{n}+\delta_\alpha) - \phi(\mathbf{n}) - a_\alpha(\mathbf{n})\right) - \frac{1}{\Gamma}\cos\left(\phi(\mathbf{n}+\delta_z) - \phi(\mathbf{n})\right)\right) \tag{3}$$

The periodic interaction function $V(\theta)$ determines the in-plane phase stiffness. The choice of the low angle asymptotics $V(\theta) \approx -1 + \theta^2/2$ fixes the energy and temperature scale to J. In most simulations $V(\theta)$ is simply taken as $-\cos(\theta)$. The influence of the grid can be reduced significantly by optimization the shape of $V(\theta)$. We chose $V(\theta)$ as $V(\theta) = -3r/4 - (1-r)\cos(\theta) - (r/4)\cos(2\theta)$, and adjust the coefficient r to minimize the energy barrier for the vortex jump to the neighbor site which gives $r = 0.37565$. The dimensionless vector potential $a_\alpha(\mathbf{n}) = (2\pi s/\Phi_0)A_\alpha$ $(\alpha = x, y, z)$ is taken in the Landau gauge $a_y(n_x) = 2\pi b n_x$, the dimensionless magnetic field $b = Bs^2/\Phi_0$ determines the fraction of the grid sites occupied by the vortices. We have used $N_\perp = 72$ and $b = 1/36$ which gives 144 vortex lines. The strength of interlayer coupling is determined by the anisotropy parameter Γ. The number of layers N_z has been varied from 4 to 40 to check for the finite size effects at different anisotropies. Most simulations were done with $N_z = 10$. The strength of coupling between the two dimensional lattices in the layers is determined by the scaled magnetic field $\Gamma s^2 B/\Phi_0 = \Gamma b$. This means that the phase diagram can be probed by varying either the field or anisotropy. Therefore the anisotropy parameter Γ should not be considered as the anisotropy of real layered superconductors but rather as a parameter which allows one to vary the scaled magnetic field. To study the thermodynamic properties, we applied the standard Metropolis algorithm. For each temperature-anisotropy point we use typically $5 \cdot 10^4$ Monte Carlo sweeps for equilibration and $(1 \div 3) \cdot 10^5$ sweeps for calculation of thermodynamic properties (up to 10^6 sweeps near phase transitions). The vortex positions are determined by a calculation of the phase circumference around each square cell α, $s_\alpha = b + \Sigma(\phi(\mathbf{n}_\alpha) - \phi(\mathbf{m}_\alpha) - a(\mathbf{n}_\alpha))$, where the sum is taken counterclockwise along four bonds surrounding a given cell. Vortices are located in the sites with $s_\alpha = 2\pi$. Fig. 1 shows a typical phase configuration and vortex positions at low temperatures. The model does not reproduce correctly the structure of vortex cores. However this structure has a very weak influence on the nature of vortex phases and the transitions between them. The model should correctly describe the thermodynamics of real superconductors at low fields and temperatures not too close to T_c, provided the filling fraction b is chosen to be small enough to minimize the influence of discretization.

The important advantage of numerical simulations is the possibility of calculating many different properties and establishing correlations between them. Properties of the system can be classified as thermodynamic properties, responses of the system to external perturbations, and properties characterizing the order in the vortex system. Thermodynamics is described by the temperature dependencies of the *internal energy* per site $U = \frac{\langle E\rangle}{N}$ with $N = N_\perp^2 N_z$ being the total number of sites. Another important thermodynamic parameter is the *average Josephson energy* $E_J = \frac{1}{\Gamma}\langle\cos\left(\phi(\mathbf{n}+\delta_z) - \phi(\mathbf{n})\right)\rangle$, which can be used as a measure of the effective coupling between neighboring layers.

The superconducting state is characterized by a nonzero value of the *superfluid response* or *helicity modulus* Q_z which determines the linear response of the supercurrent to the external vector potential A_{ext}, $j_z = Q_z A_{ext}$. The thermodynamic expression for Q_z is given by [6]

$$Q_z = \frac{\langle \sum_{\mathbf{n}} \cos\left(\phi(\mathbf{n}+\delta_z) - \phi(\mathbf{n})\right)\rangle}{N\Gamma} - \frac{\left\langle \left[\sum_{\mathbf{n}} \sin\left(\phi(\mathbf{n}+\delta_z) - \phi(\mathbf{n})\right)\right]^2 \right\rangle - \left\langle \sum_{\mathbf{n}} \sin\left(\phi(\mathbf{n}+\delta_z) - \phi(\mathbf{n})\right)\right\rangle^2}{TN\Gamma^2} \qquad (4)$$

We will characterize the order in the vortex lattice by *the concentration of lattice defects* n_{def} obtained by the Delauney triangulation (fraction of particles with the coordination numbers different from 6) and the in-plane density correlation function. Alignment of pancake vortices can be characterized by the density correlation function for adjacent points belonging to neighboring layers $g_{al} = \langle \rho(\mathbf{n})\rho(\mathbf{n}+\delta_z)\rangle / b$. We will refer to g_{al} as *the alignment parameter.*

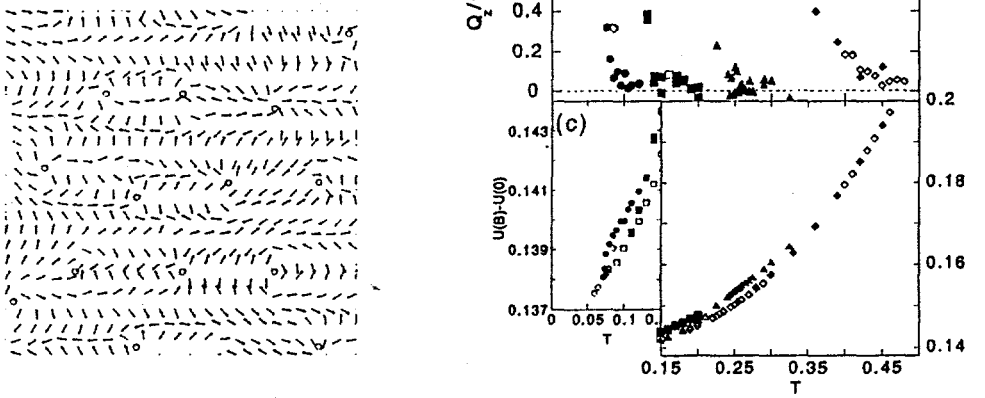

FIG. 1. Typical phase and vortex configuration at low temperatures. Phases at the sites of grid are represented by the tilting angles of arrows

FIG. 2. Temperature dependencies of the defect concentration n_{def} (a), superfluid response Q_z(b), and excess internal energy $U(B) - U(0)$(c) at different anisotropies Γ (scaled magnetic fields). The number of layers is 4 for $\Gamma = 800$ and 10 for other values of Γ

RESULTS AND DISCUSSION

We studied the temperature dependence of various parameters at different values of the anisotropy parameter Γ. Figure 2 shows plots of the defect concentration n_{def}, the superfluid response Q_z, and the difference between the internal energy per site U and the internal energy in the Meissner state $U(0) = -2 - 1/\Gamma + 0.5T$. The melting of the lattice manifests itself as a steep increase of n_{def} in narrow temperature range, which is accompanied by a jump in U. The behavior near the melting transition is hysteretic. Nevertheless, slowly cooling the system does produce the triangular lattice of aligned pancake vortices. The lattice is usually incommensurate with the numerical grid and contains a small amount of frozen dislocations. Different cooling circles produce vortex lattices oriented at different angles with respect to the grid. As one can see from Fig. 2 at least two types of behavior can be distinguished depending upon the anisotropy parameter. At high anisotropies the system looses the crystalline order simultaneously with superconductivity along the field direction as a result of the strong first order phase transition. The melting transition is accompanied by a

strong suppression of pancake alignment. Nevertheless, the influence of the interlayer coupling on the melting transition persists up to surprisingly high anisotropies. For example, for $\Gamma = 800$, corresponding to $B = 22.2B_{cr}$, melting still takes place at the temperature 1.5 times higher than the melting temperature of single 2D layer T_m^{2D} [16](in our units $T_m^{2D} = 0.045$). At lower anisotropies the melting transition becomes weaker. Above the melting temperature the pancake vortices in different layers are still strongly aligned so that the vortex lines can be easily traced. This phase is characterized by the superconductivity along the field, as was first observed in Ref. [6]. The transition between these two regimes takes place at $B \approx (3 \div 5)B_{cr}$. Alignment of pancakes in neighbor layers can be quantitatively characterized by the "alignment parameter" g_{al} defined in previous Section. Fig. 3 shows the temperature dependencies of this parameter at different Γ. As one can see, the melting transition at high anisotropy is indeed accompanied by steep drop of pancake alignment, indicating a transition into the pancake liquid state. In contrast, at low anisotropies the pancake alignment does not show any singularity at the melting point and decreases smoothly with the increase of temperature. The internal energy U experiences a jump ΔU at the melting transition. The strength of the first order transition can be characterized by the entropy jump per vortex per layer ΔS, $\Delta S = \Delta U/(bT_m)$ [7]. We found that at high anisotropies (high fields) this parameter is large (0.3-0.4 k_B/ pancake), indicating a strong transition. At low anisotropies, in the line melting regime, ΔS steeply drops to very small values (< 0.05 k_B/pancake). Such small values are in agreement with the entropy jumps for the *crystal → line liquid* transition obtained in the model of interacting lines [5] and in the lowest Landau level approximation [14]. The field dependence of the entropy jump is shown in Fig. 4.

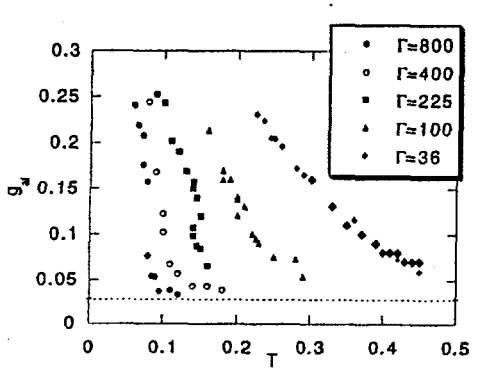

FIG. 3. Temperature dependencies of the alignment parameter for different anisotropies. Dashed horizontal line $g_{al} = b$ corresponds to completely misaligned pancake liquids in neighbor layers.

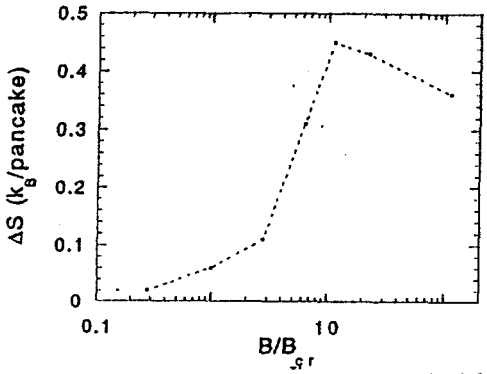

FIG. 4. Field dependence of the entropy jump at the melting transition

To check for the universality suggested by Eq. (2), we performed simulations for two different sets of parameters preserving the same ratio B/B_{cr} (system size, anisotropy and field have been taken as 72x72x10, 100, 1/36 and 128x128x16, 178, 1/64). Fig. (5) shows temperature dependence of the defect concentrations and helicity modulus for these systems. One can see that both parameters have an almost identical the temperature dependence and the melting transitions occur at exactly the same point. This confirms an universality of the phase diagram plotted in the reduced variables. Simulation results are summarized in the field-temperature phase diagram (Fig. 6). At fields $> 3B_{cr}$, the melting line separates the vortex crystal and the pancake liquid phases. At lower fields the crystalline state transfers into the intermediate line liquid state which becomes normal at higher temperatures.

ACKNOWLEDGEMENTS

I would like to thank Prof. S.Teitel and Prof. Z.Tešanović for illuminating discussions and L.Paulius for reading the manuscript and useful comments. This work was supported by the National Science Foundation Office of the Science and Technology Center under contract No. DMR-91-20000. and by the U. S. Department of Energy, BES-Materials Sciences, under contract No. W-31- 109-ENG-38. The author gratefully acknowledge use of the Argonne High-Performance Computing Research Facility. The HPCRF is funded principally by the U.S. Department of Energy Office of Scientific Computing.

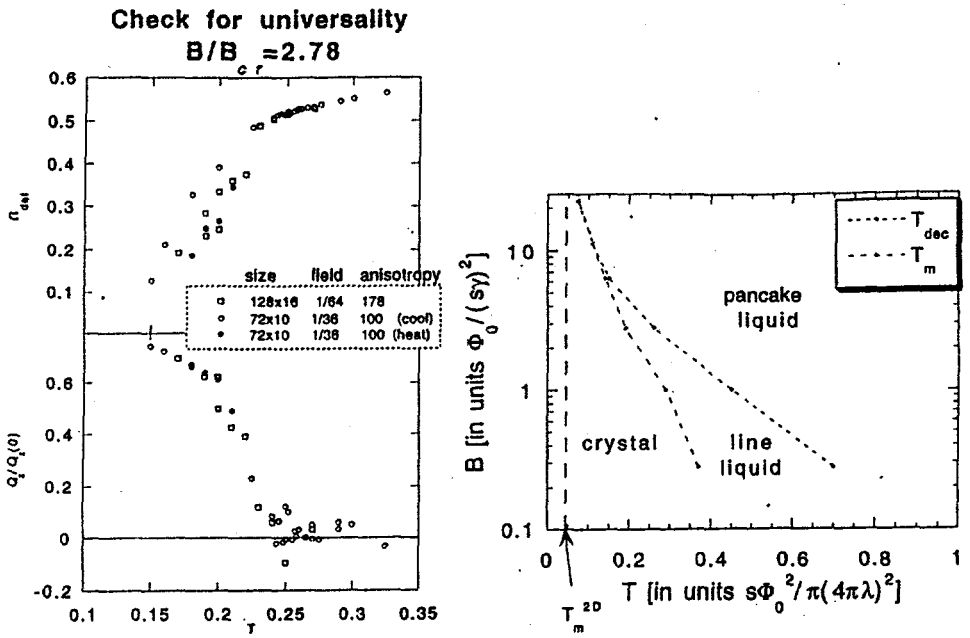

FIG. 5. Check for universality of phase diagram: temperature dependencies of defect concentration and superconducting response for two different simulation systems with the same ratio $B/B_{cr} = 2.78$.

FIG. 6. Field-temperature phase diagram obtained from simulations

REFERENCES

[1] M.V.Feigel'man *et al*, Phys. Rev. B, **48**, 16641 (1994)

[2] Z.Tešanović, Phys. Rev. B, **51**, 16204 (1995)

[3] H. Safar *et al*, Phys. Rev. Lett. **69**, 824 (1992);W. K. Kwok *et al*, Phys. Rev. Lett. **72**, 1092 (1994)

[4] E. Zeldov *et al* Nature **375**, 373 (1995); U. Welp *et al*, Phys. Rev. Lett.,??, ??? (1996)

[5] S.Ryu *et al*, Phys. Rev. Lett., **68**, 710 (1992); S.Ryu and D.Stroud, Phys. Rev. B, **54**, 1320 (1996)

[6] Y.-H.Li and S.Teitel, Phys. Rev. B, **47**, 359 (1993), Phys. Rev. B, **49**, 4136 (1994).

[7] R.E.Hetzel, A.Subdø, and D.A.Huse, Phys. Rev. Lett., **69**, 518 (1992)

[8] T.Chen and S.Teitel, unpublished

[9] E.A.Jagla and C.A.Balseiro, Phys. Rev. B, **53**, R538 (1996); Phys. Rev. B,**52**, 4494 (1995)

[10] D.Dominguez, N.Grønbech-Jensen, and A.R.Bishop, Phys. Rev. Lett., **75**, 4670 (1995)

[11] R.Cavalcanti, G.Carneiro, and A.Gartner, Europhys. Lett. **17**, 449 (1992); G.Carneiro, R.Cavalcanti, and A.Gartner, , **47**, 5263 (1993);G.Carneiro, Phys. Rev. Lett., **75**, 521 (1995)

[12] T.Chen and S.Teitel, Phys. Rev. Lett., **74**, 2792 (1996)

[13] A.K.Nguyen, A.Subdø, and R.E.Hetzel, preprint, cond-mat/9606002

[14] R.Šášik and D.Stroud Phys. Rev. Lett., **72**, 2462 (1994)

[15] J.Hu and A.H.MacDonald, unpublished

[16] J.M.Caillol *et al* Journal of Stat.Phys., 28, 325(1982); S.A.Hattel and J.M.Wheatley, Phys. Rev. B, **50**, 16590 (1995);*ibid* **51**, 11951 (1995); M.Franz and S.Teitel, Phys. Rev. Lett., **75**, 521 (1995)